CENTRAL BOUQUET HEMORRHAGE

Clinical and Multimodal Imaging Features

PRITHVI RAMTOHUL, MD,* ADRIAN AU, MD, PHD,† ANNE L. KUNKLER, MD,‡ TOMMASO BACCI, MD,§ ROSA DOLZ-MARCO, MD, PHD,¶ ROBERTO GALLEGO-PINAZO, MD, PHD,¶ NICOLAS YANNUZZI, MD,‡ DAVID SARRAF, MD,† K. BAILEY FREUND, MD***

Purpose: To describe the clinical characteristics, multimodal imaging features, and anatomic basis of a distinctive pattern of deep retinal hemorrhages located in the central fovea, a presentation referred to as "central bouquet hemorrhage."

Methods: Retrospective, observational, multicenter case series of eyes with central bouquet hemorrhage. Multimodal imaging features were reviewed and analyzed.

Results: Ten eyes from 10 patients (4 women and 6 men), with a mean age of 55.6 ± 21.7 years (range 25–84 years) were included. Underlying etiologies were neovascular age-related macular degeneration (40%), lacquer cracks in pathological myopia (30%), macular telangiectasia Type 2 (10%), proliferative diabetic retinopathy (10%), and ocular trauma associated with angioid streaks (10%). On ophthalmoscopy, all eyes with central bouquet hemorrhage displayed a deep retinal hemorrhage with round margins in the central fovea and associated with petaloid hemorrhages radiating in the surrounding Henle fiber layer. Cross-sectional optical coherence tomography showed a well-delineated round hyperreflective lesion involving the central foveal Henle fiber layer/outer nuclear layer in all cases. Accompanying hyperreflective hemorrhages tracking along the obliquely oriented Henle fiber layer were present in all eyes. Resolution occurred in all patients, either spontaneously (30%) or after treatment with intravitreal anti-vascular endothelial growth factor injections (70%), and was associated with partial visual acuity improvement (from 20/113 to 20/36).

Conclusion: "Central bouquet hemorrhage" is a novel descriptive term describing a characteristic round pattern of intraretinal blood in the fovea associated with Henle fiber layer hemorrhage and encountered in a spectrum of macular disease.

RETINA 44:551–557, 2024

The Rochon-Duvigneaud's "bouquet des cones centraux" (central bouquet, CB) refers to a small circular island measuring 100 to 200 μm in diameter that comprises densely packed cone photoreceptors and a specialized population of glial elements called Müller cell cones.[1–5] The CB is characterized by unique geometry and morphology of cone photoreceptors including thin elongated inner (i.e., myoid and ellipsoid) and outer segments, packed cell bodies distributed in up to six layers, and short vertically oriented axons connecting their synaptic pedicles in the foveal pit floor.[6,7] The Henle fiber layer (HFL) is formed by the outer processes of Müller cell cones which accompany the cone axons.[8] These processes terminate at the boundary between the cone cell bodies and myoids by continuous heterotypic adherens junctions that collectively form the external limiting membrane (ELM).[8,9]

Accumulation of blood within the perifoveal HFL may result in a specific pattern of intraretinal hemorrhage known as *HFL hemorrhage*.[10] This type of hemorrhage is characterized by a petaloid or radial distribution displaying a feathery edge on ophthalmoscopy and

From the *Vitreous Retina Macula Consultants of New York, New York, New York; †Retinal Disorders and Ophthalmic Genetics Division, Stein Eye Institute, University of California Los Angeles, Los Angeles, California; ‡Department of Ophthalmology, Bascom Palmer Eye Institute, Miller School of Medicine, University of Miami, Miami, Florida; §Ophthalmology Unit, Department of Medicine, Surgery and Neuroscience, University of Siena, Siena University Hospital, Siena, Italy; ¶Unit of Macula, Oftalvist Clinic, Valencia, Spain; and **Department of Ophthalmology, NYU Grossman School of Medicine, New York, New York.

Supported by The Macula Foundation Inc., New York, New York, USA. Prithvi Ramtohul was supported by the Philippe Foundation.

K.B. Freund is a consultant for Heidelberg Engineering, Zeiss, Allergan, Bayer, Genentech, and Novartis. D. Sarraf is a consultant for Amgen, Genentech-Roche, Heidelberg, Novartis, Optovue, Regeneron, Bayer, and Topcon. The other authors report no disclosures.

Reprint requests: K. Bailey Freund, MD, Vitreous Retina Macula Consultants of New York, 950 Third Ave., New York, NY 10022; e-mail: kbfreund@gmail.com

hyperreflective changes separated by hyporeflective oblique septa on optical coherence tomography (OCT).[10] These HFL hemorrhages are often found in patients with systemic or ocular venous anomalies and originate predominantly from the adjacent deep capillary plexus (DCP).[10,11] We have observed a peculiar pattern of HFL hemorrhage involving the CB, a presentation referred to as "CB hemorrhage" (CBH). In the existing literature, instances of CBH have been documented.[12–14] However, as far as we know, there has been no elucidation of the anatomical basis of this pattern nor a differentiation between HFL hemorrhage cases with and without CBH.

This study aims to describe the clinical and multimodal imaging features of CBH, to elucidate its anatomic location and to discuss the potential implications.

Methods

This is an observational, retrospective, multicenter case series of patients presenting with CBH. Each coauthor identified compatible cases using patient lists, keywords, or diagnostic indicators applied to their database from 2018 to 2022. This study was approved by the Western Institutional Review Board-Copernicus Group (Princeton, NJ), and written informed consent was not required because of the retrospective nature of this study. This report adhered to the tenets of the Declaration of Helsinki and complied with the Health Insurance Portability and Accountability Act.

The inclusion criteria were eyes with findings on clinical examination and multimodal imaging consistent with CBH, defined as a deep retinal hemorrhage with round margins centered on the fovea with varying amounts of adjacent petaloid hemorrhage radiating in the surrounding HFL and corresponding to a central hyperreflective intraretinal lesion on OCT.

All patients underwent a complete ophthalmologic examination, including measurement of the best-corrected visual acuity (BCVA) using Snellen charts, slitlamp biomicroscopy, and indirect fundus ophthalmoscopy. Multimodal retinal imaging was reviewed and studied when available including color fundus photography (EIDON AF, Centervue Padova, Italy or Topcon TRC-50IX retinal camera, Topcon Medical Systems, Oakland, NJ or Optos plc, Dunfermline, Scotland), spectral domain OCT (OCT; Spectralis, Heidelberg Engineering, Heidelberg, Germany, or CIRRUS 6000, Carl Zeiss Meditec, Inc, Dublin, CA), high-resolution spectral domain OCT (High-Res OCT prototype, Heidelberg Engineering, Heidelberg, Germany), swept source OCT and OCT angiography (PLEX Elite 9000, Carl Zeiss Meditec, Inc), fundus autofluorescence (Spectralis HRA, Heidelberg Engineering or Optos, plc), and fluorescein angiography (Spectralis HRA, Heidelberg Engineering or Optos, plc).

Detailed chart reviews were performed, and deidentified demographic and clinical data, including age, sex, refraction, presenting symptoms, ocular and systemic medical history, ocular and systemic therapies, and baseline and final Snellen BCVA, were collected and summarized. The Snellen BCVA was converted to logarithm of minimum angle of resolution for analysis. Quantitative and qualitative data are presented as mean ± SD and median, and absolute and relative proportions, respectively.

Results

Demographic Data

Ten eyes from 10 patients (4 women and 6 men) were included. The mean age of the cohort was 55.6 ± 21.7 years (range 25–84 years; median, 59.0 years), and the mean follow-up duration was 45.6 months (range 12–204 months; median, 12.0 months). Seven eyes (70%) were emmetropic, and three eyes (30%) were highly myopic with a mean spherical equivalent of −13.6 diopters (range −15.0 to −12.0 diopters). Involvement was unilateral in all cases. At presentation, the mean BCVA was 0.76 logarithm of minimum angle of resolution (Snellen equivalence, 20/115; range 20/40–20/350). Seven patients (70%) were treated with intravitreal injections of anti-vascular endothelial growth factor, and the mean number of injections was 3 (range 1–6; median 3 injections). Three patients (30%) were observed.

Presenting symptoms were acute vision loss with central scotoma in all cases. Systemic medical history included hypertension (40%), diabetes mellitus (20%), dyslipidemia (10%), obstructive sleep apnea (10%), and pseudoxanthoma elasticum (10%). Ocular medical history included neovascular age-related macular degeneration (nAMD, 30%), lacquer cracks secondary to pathological myopia (30%), ruptured retinal arterial macroaneurysm (10%), macular telangiectasia Type 2 (10%), proliferative diabetic retinopathy (10%), and ocular blunt trauma associated with pre-existent angioid streaks (10%). Table 1 summarizes the demographic and clinical data.

Ophthalmoscopic Features

On ophthalmoscopic examination, CBH was characterized by a deep retinal hemorrhage with round margins centered on the fovea. Surrounding HFL

Table 1. Demographic and Clinical Data of Patients With Central Bouquet Hemorrhage

Characteristics	Number
No. of patients	10
No. of eyes	10
Age (mean years ± SD)	55.6 ± 21.7
Follow-up duration (mean months, range)	45.6 (12–204)
Sex, n (%)	
Male	6/10 (60.0)
Female	4/10 (40.0)
Refractive error n (%)	
Highly myopic	3/10 (30.0)
Emmetropic	7/10 (70.0)
BCVA in logMAR (mean Snellen equivalent)	
Initial	0.76 (20/115)
Final	0.26 (20/36)
Underlying etiologies n (%)	
nAMD	3/10 (30.0)
Lacquer cracks	3/10 (30.0)
Ruptured retinal arterial macroaneurysm	1/10 (10.0)
MacTel 2	1/10 (10.0)
Proliferative diabetic retinopathy	1/10 (10.0)
Ocular Trauma and angioid Streaks	1/10 (10.0)
Treatments n (%)	
Intravitreal anti-VEGF injections	7/10 (70.0)
Observation	3/10 (30.0)

LogMAR, logarithm of minimum angle of resolution; MacTel 2, macular telangiectasia Type 2; VEGF, vascular endothelial growth factor.

hemorrhages located in the perifoveal macula were seen in all cases and displayed the typical petaloid distribution radiating from the fovea. Associated subretinal fluid and hemorrhage were noted in eight eyes (80%, three eyes with nAMD, three eyes with pathological myopia, one eye with ruptured retinal arterial macroaneurysm, and one eye with angioid streaks).

Multimodal Imaging Features

On cross-sectional OCT, CBH corresponded to a hyperreflective lesion within the central foveal HFL and outer nuclear layer (ONL) and bordered posteriorly by the ELM in all cases. The shape of CBH varied with the volume of accumulated blood and was categorized into two patterns: 1) smaller CBH (mean horizontal diameter, 85.5 μm) displayed a truncated cone appearance (80% of eyes), while 2) larger CBH (mean horizontal diameter, 282.7 μm) displayed a piriform or hemispherical-shaped configuration with acute angles at the base (20% of eyes). Surrounding hyperreflective radial HFL hemorrhages located in the perifovea were identified in all cases. The foveal ellipsoid zone (EZ) and interdigitation zone were disrupted in all cases. Subretinal fluid and hemorrhages were present in 80% of eyes.

With en face OCT segmented at the level of the outer retina, CBH was characterized by a hyperreflective round-shaped lesion centered on the fovea and bordered by a thin hyperreflective edge in all cases. Adjacent hyperreflective HFL hemorrhages displayed a petaloid pattern radiating from the fovea in all cases.

On fundus autofluorescence and fluorescein angiography, CBH showed blocked hypoautofluorescence and hypofluorescence, respectively. On OCT angiography, CBH colocalized with macular neovascularization in three eyes (30%), telangiectasias and microaneurysms around the foveal avascular zone in two eyes (20%), and no apparent abnormalities were noted in the remaining eyes (40%). Figure 1 shows representative cases of CBH on multimodal imaging.

Evolution and Complications

During the follow-up period, resolution of CBH occurred in all cases (mean duration: 10 ± 4 weeks) either spontaneously (three patients) or concurrent with intravitreal anti-vascular endothelial growth factor injections in seven patients and was associated with visual acuity improvement (final mean BCVA, 0.26 logarithm of minimum angle of resolution; Snellen equivalence, 20/36; range, 20/20–20/50) at the end of the follow-up. On cross-sectional OCT, regression of CBH was followed by vertical hyperreflective lesions tracking along the central HFL/ONL in 80% of eyes. Final alterations of the central EZ/interdigitation zone were noted in all cases. No significant thinning of the HFL/ONL was observed after complete regression of the CBH. Figure 2 shows the serial multimodal imaging of CBH associated with nAMD. None of the cases developed full-thickness macular hole.

Discussion

In this report, we describe a series of patients with a deep intraretinal hemorrhage in the central fovea corresponding to a hyperreflective conical lesion within the HFL/ONL on OCT. All cases were unilateral and associated with radial HFL hemorrhages in the perifovea displaying a characteristic petaloid pattern. We postulate that these specific morphologic features and OCT localization are related to the anatomy of the CB and the vertical pathway of Müller cells in the central fovea,[15] and therefore, we suggest the term *central bouquet hemorrhage* to describe this clinical presentation.

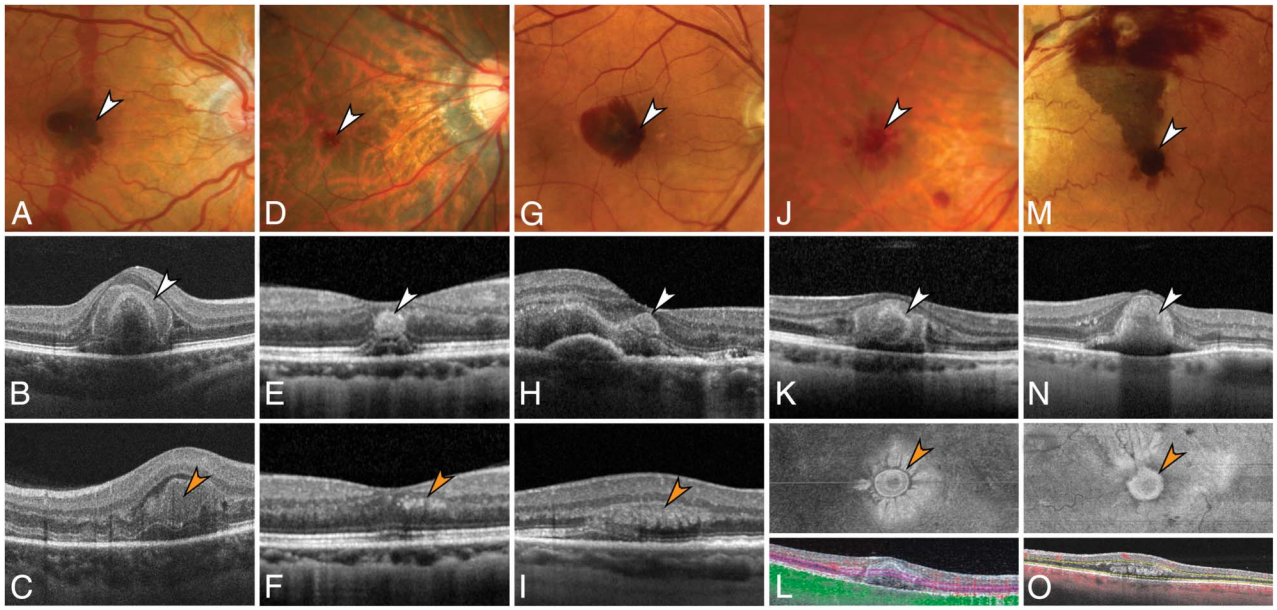

Fig. 1. Representative cases of CBH on multimodal imaging. **A–C.** Case 1. A man in his 20s with angioid streaks and ocular trauma. **A.** Color fundus photography of the right eye shows a deep round-shaped CBH centered by the fovea (*white arrowhead*). Note the HFL hemorrhages with a feathery edge and petaloid distribution that surround the CBH. **B.** Horizontal OCT B scan through the fovea shows a piriform-shaped hyperreflective CBH with acute angles at the base (*white arrowhead*). The CBH is located in the central foveal HFL/ONL. Note the presence of subretinal fluid/hemorrhage. **C.** Vertical OCT B scan though the nasal fovea shows concurrent HFL hemorrhages (*orange arrowhead*). **D–F.** Case 2. Myopic woman (−12.0 diopters) in her 20s with lacquer cracks. **D.** Color fundus photography of the right eye shows a small, deep, round-shaped CBH centered by the fovea (*white arrowhead*). **E.** Horizontal OCT B scan through the fovea shows a conical hyperreflective CBH (*white arrowhead*). The CBH is located in the central foveal HFL/ONL and is posteriorly bordered by the ELM. **F.** Adjacent OCT B scan though the inferior fovea shows concurrent HFL hemorrhages (*orange arrowhead*). **G–I.** Case 3. A man in his 80s with neovascular age-related macular degeneration. **G.** Color fundus photography of the right eye shows a deep round-shaped CBH centered by the fovea (*white arrowhead*). Note the HFL hemorrhages with a feathery edge and petaloid distribution that surround the CBH. **H.** Horizontal OCT B scan through the fovea shows a conical hyperreflective CBH (*white arrowhead*). The CBH is located in the central foveal HFL/ONL and is posteriorly bordered by the ELM. Note the presence of subretinal fluid/hemorrhage and a pigment epithelial detachment. **I.** Adjacent OCT B scan though the inferior fovea shows concurrent HFL hemorrhages (*orange arrowhead*). **J–L.** Case 4. Myopic woman (−14.0 diopters) in her 20s with lacquer cracks. **J.** Color fundus photography of the right eye shows a deep round-shaped CBH centered by the fovea (*white arrowhead*). Note the HFL hemorrhages with a feathery edge and petaloid distribution that surround the CBH. **K.** Horizontal OCT B scan through the fovea shows a piriform-shaped hyperreflective CBH (*white arrowhead*). The CBH is located in the central foveal HFL/ONL. Note the presence of subretinal fluid. **L.** En face OCT segmented at the level of the HFL/ONL shows a round-shaped hyperreflective CBH centered by the fovea and bordered by a thin hyperreflective edge (*orange arrowhead*). Adjacent hyperreflective HFL hemorrhages exhibit a petaloid pattern radiating from the fovea. The inset is the corresponding OCT B scan with the purple lines indicating the segmentation used to obtain the image in (**L**). **M–O.** Case 5. A man in his 60s with ruptured retinal arterial macroaneurysm. **M.** Color fundus photography of the left eye shows a deep round-shaped CBH centered by the fovea (*white arrowhead*). Note the HFL hemorrhages with a feathery edge and petaloid distribution that surround the CBH. **N.** Horizontal OCT B scan through the fovea shows a piriform-shaped hyperreflective CBH (*white arrowhead*). The CBH is located in the central foveal HFL/ONL. Note the presence of subretinal fluid. **O.** En face OCT segmented at the level of the HFL/ONL shows a round-shaped hyperreflective CBH centered by the fovea and bordered by a thin hyperreflective edge (*orange arrowhead*). Adjacent hyperreflective HFL hemorrhages exhibit a petaloid pattern radiating from the fovea. The inset is the corresponding OCT B scan with the yellow lines indicating the segmentation used to obtain the image in (**N**).

The advent of high-resolution retinal imaging modalities, especially spectral domain OCT, has enabled in vivo visualization of CB abnormalities in retinal conditions, including tractional macular disorders and cystoid macular edema.[16,17] Notably, the presence of CB abnormalities on OCT has clinical and prognostic implications. For example, morphological CB alterations identified with OCT in eyes with epiretinal membrane, including "the cotton ball sign", foveolar detachment, and acquired vitelliform lesions, correlate with reduced visual function.[16,18] Moreover, CB abnormalities are associated with worse visual outcomes after epiretinal membrane surgery.[19] However, most OCT studies have focused their analyses on the posterior aspects of the CB, namely the central EZ/interdigitation zone. In this study, we described accumulation of hemorrhage within the anterior portion of the CB. Importantly, the occurrence of CBH also had clinical and prognostic implications because regression was followed by incomplete visual acuity restoration and persistent alterations of the central foveal EZ/interdigitation zone in all cases.

Based on the underlying etiologies and the consistent association with perifoveal HFL hemorrhages, two distinctive pathways of CBH formation may be suggested: 1) an anterior pathway involving the diffusion of blood from the choroid and 2) a posterior pathway of blood diffusion from the DCP. In fact,

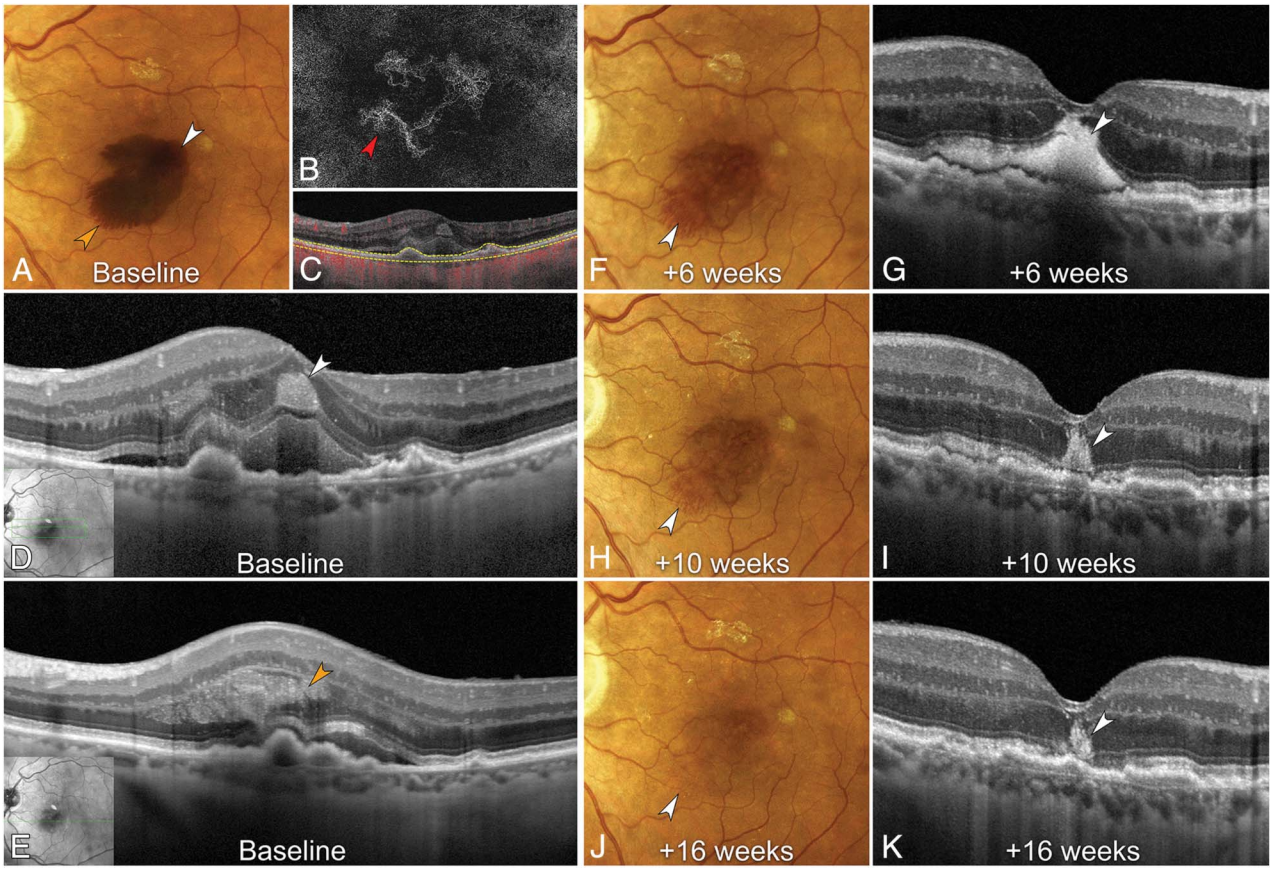

Fig. 2. Longitudinal multimodal imaging of CBH associated with neovascular age-related macular degeneration. **A.** Baseline confocal fundus photography of the left eye shows a deep round-shaped CBH centered by the fovea (*white arrowhead*) and surrounded by HFL hemorrhages with a typical feathery edge (*orange arrowhead*). The time point is displayed. **B.** En face OCTA segmented between the retinal pigment epithelium and Bruch membrane shows a macular neovascularization (*red arrowhead*). **C.** Corresponding OCTA B scan with the yellow lines indicating the segmentation used to obtain the image in (**B**). **D.** High-resolution (high-Res) OCT B scan shows a conical hyperreflective CBH (*white arrowhead*). The CBH is located in the central foveal HFL/ONL and is posteriorly bordered by the ELM. Note the presence of subretinal fluid/hemorrhage and a shallow irregular pigment epithelial detachment. The inset is the near infrared reflectance image with the green line indicating the position of the high-Res OCT B scan. The timepoint is displayed. **E.** Adjacent high-Res OCT B scan though the inferior fovea shows concurrent HFL hemorrhages (*orange arrowhead*). The inset is the near infrared reflectance image with the green line indicating the position of the high-Res OCT B scan. The time point is displayed. **F.** At 6 weeks of follow-up, confocal fundus photography shows gradual fading of the CBH and HFL hemorrhages (*white arrowhead*). The time point is displayed. **G.** At 6 weeks of follow-up, tracked high-Res OCT B scan shows regression of the hyperreflective CBH located in the central foveal HFL/ONL and bordered posteriorly by the ELM (*white arrowhead*). Note the persistent subretinal hyperreflective hemorrhage. The time point is displayed. **H.** At 10 weeks of follow-up, confocal fundus photography shows gradual fading of the CBH and HFL hemorrhages (*white arrowhead*). The time point is displayed. **I.** At 10 weeks of follow-up, tracked high-Res OCT B scan shows persistent vertical hyperreflective CBH tracking along the central foveal HFL/ONL and bordered posteriorly by the ELM (*white arrowhead*). Note the resolution of the subretinal hemorrhage. The time point is displayed. **J.** At 16 weeks of follow-up, confocal fundus photography shows complete regression of the CBH and HFL hemorrhages (*white arrowhead*). The time point is displayed. **K.** At 16 weeks of follow-up, tracked high-Res OCT B scan shows persistent vertical hyperreflective CBH tracking along the central foveal HFL/ONL and bordered posteriorly by the ELM (*white arrowhead*). Note the persistent disruption of the central ellipsoid and interdigitation zones. The time point is displayed.

hemorrhage from the choroid (e.g., macular neovascularization, myopic lacquer cracks) has been associated with perifoveal HFL hemorrhages.[10] Notably, cases of CBH in highly myopic eyes have been reported in the literature, although the interpretation of blood localization on OCT is inconsistent.[12–14] Abnormal hemodynamic forces resulting from choroidal leakage and disruption of the foveal ELM may contribute to the anterograde tracking of blood within the CB.[9] This mechanism is supported by the high prevalence of subretinal fluid/hemorrhage (80%) and preexistent outer retinal disruption (e.g., nAMD, pathological myopia, angioid streaks) seen in this subgroup in our study. Moreover, disruption of the DCP and diffusion of blood into the adjacent HFL have been reported in eyes with elevated central and local venous pressure.[10,11] In fact, the DCP is the major site of retinal venous drainage based on confocal microscopy and retinal imaging studies using OCT angiography and fluorescein angiography.[20,21] The hydraulic conductivity of human retinas has been assessed by Antcliff et al, who demonstrated that fluid leakage from the

DCP is restrained by two high-resistance barriers: The inner plexiform layer composed of dense dendritic processes of bipolar, amacrine and ganglion cells, and the outer plexiform layer consisting of invaginated rod and cone synapses.[22,23] Therefore, blood leakage from the damaged DCP primarily extends into the HFL/ONL, causing displacement of photoreceptor axons and nuclei.[24]

Accurate assessment of the retinal hemorrhage location, whether intraretinal or subretinal, is fundamental as the detection of blood can be used as a surrogate endpoint in neovascular AMD trials and may affect distinct treatment strategies, visual prognosis, and pathogenic pathways.[25] The main differential diagnoses of CBH include central subretinal hemorrhage and hemorrhagic bacillary layer detachment (BALAD).[26] The hemorrhagic variant of BALAD was first described by Ramtohul et al in a case of proliferative macular telangiectasia Type 2, and subsequent studies reported this OCT finding in nAMD and ruptured retinal arterial macroaneurysms.[27–29] On OCT, hemorrhagic BALAD is characterized by accumulation of hyperreflective blood within the cavity formed by the BALAD (i.e., split at the level of the photoreceptor inner segment myoids).[26,27] Its anterior border is marked by the ELM, and the posterior border is represented by a faint EZ corresponding to residual inner and outer segments remaining adherent to the retinal pigment epithelium/Bruch membrane complex.[26–28] Conversely, CBH is characterized on OCT by the accumulation of hyperreflective blood within the central foveal HFL/ONL with the posterior border being the ELM. Furthermore, the clinical course of hemorrhagic BALAD and CBH is distinct: while hemorrhagic BALAD tends to resolve rapidly after intravitreal injections of anti-vascular endothelial growth factor, as shown in previous studies, CBH may persist for several weeks with a legacy of vertical hyperreflective lesions tracking along the central foveal HFL/ONL.[26–28] Moreover, regressing CBH may masquerade as hyperreflective lesions affecting the central foveal HFL/ONL, including retinal pigment epithelium plume, vertical hyperreflective lesions associated with vitreoretinal lymphoma or viral retinitis, vertical hyperreflective stress lines, foveal outer retinal hyperreflectivity, and the angular sign of HFL hyperreflectivity.[8,30]

Strengths of our study include the detailed characterization of CBH using multimodal imaging techniques, the use of high-resolution OCT prototype with increased axial resolution enabling accurate localization of blood within the retinal layers, the correlation of OCT-derived anatomical information with previously published histologic data of human foveae, and the validation of a novel descriptive terminology based on the seminal descriptions provided by Rochon-Duvigneaud. Limitations include the small number of patients and the lack of complete multimodal imaging data in some cases.

In conclusion, CBH is a novel descriptive terminology referring to the accumulation of blood within the central foveal HFL/ONL. Specific morphologic features, localization, and clinical course characterize this pattern of intraretinal hemorrhage. Diffusion of blood from the choroidal vasculature or the DCP may account for the variety of underlying etiologies.

Key words: central foveal bouquet, hemorrhage, Henle fiber layer, multimodal imaging, optical coherence tomography, Rochon-Duvigneaud.

References

1. Polyak SL. The Retina: The Anatomy and the Histology of the Retina in Man, Ape, and Monkey: Including the Consideration of Visual Functions, the History of Physiological Optics, and the Histological Laboratory Technique. Chicago, IL: The University of Chicago Press; 1941.
2. Rochon-Duvigneaud A. Recherches sur la fovea de la rétine humaine et particulièrement sur le bouquet des cônes centraux. Arch Anat Microsc 1907;9:315–342.
3. Hendrickson AE, Yuodelis C. The morphological development of the human fovea. Ophthalmology 1984;91:603–612.
4. Gass JD. Müller cell cone, an overlooked part of the anatomy of the fovea centralis: hypotheses concerning its role in the pathogenesis of macular hole and foveomacualr retinoschisis. Arch Ophthalmol 1999;117:821–823.
5. Yamada E. Some structural features of the fovea centralis in the human retina. Arch Ophthalmol 1969;82:151–159.
6. Curcio CA, Messinger JD, Sloan KR, et al. Human chorioretinal layer thicknesses measured in macula-wide, high-resolution histologic sections. Invest Ophthalmol Vis Sci 2011;52:3943–3954.
7. Cuenca N, Ortuño-Lizarán I, Pinilla I. Cellular characterization of OCT and outer retinal bands using specific immunohistochemistry markers and clinical implications. Ophthalmology 2018;125:407–422.
8. Ramtohul P, Cabral D, Sadda S, et al. The OCT angular sign of Henle fiber layer (HFL) hyperreflectivity (ASHH) and the pathoanatomy of the HFL in macular disease. Prog Retin Eye Res 2023;95:101135.
9. Omri S, Omri B, Savoldelli M, et al. The outer limiting membrane (OLM) revisited: clinical implications. Clin Ophthalmol 2010;4:183–195.
10. Baumal CR, Sarraf D, Bryant T, et al. Henle fibre layer haemorrhage: clinical features and pathogenesis. Br J Ophthalmol 2021;105:374–380.
11. Au A, Hou K, Baumal CR, Sarraf D. Radial hemorrhage in Henle layer in macular telangiectasia type 2. JAMA Ophthalmol 2018;136:1182–1185.
12. Lane RG, Nelson ML, Belmont JB. Petalloid foveal hemorrhage in a patient with high myopia. Arch Ophthalmol 2004;122:660–661.
13. Asai T, Ikuno Y, Nishida K. Macular microstructures and prognostic factors in myopic subretinal hemorrhages. Invest Ophthalmol Vis Sci 2014;55:226–232.

14. Mazzola M, Premoli L, Metrangolo C, et al. Myopic simple hemorrhage presenting as radial hemorrhage in Henle's fiber layer. Case Rep Ophthalmol 2021;12:446–450.
15. Bringmann A, Syrbe S, Görner K, et al. The primate fovea: structure, function and development. Prog Retin Eye Res 2018; 66:49–84.
16. Govetto A, Bhavsar KV, Virgili G, et al. Tractional abnormalities of the central foveal bouquet in epiretinal membranes: clinical spectrum and pathophysiological perspectives. Am J Ophthalmol 2017;184:167–180.
17. Lenis TL, Au A, Hou K, et al. Alterations of the foveal central bouquet associated with cystoid macular edema. Can J Ophthalmol 2020;55:301–309.
18. Iovino C, Ramtohul P, Au A, et al. Vitelliform maculopathy: diverse etiologies originating from one common pathway. Surv Ophthalmol 2023;68:361–379.
19. Brinkmann MP, Michels S, Brinkmann C, et al. Epiretinal membrane surgery outcome in eyes with abnormalities of the central bouquet. Int J Retina Vitreous 2021;7:7.
20. Ramtohul P, Iovino C, Au A, et al. Clinical and morphologic characteristics of perivenular fernlike leakage on ultrawide-field fluorescein angiography. Ophthalmol Retina 2022;6: 1070–1079.
21. An D, Yu P, Freund KB, et al. Three-dimensional characterization of the normal human parafoveal microvasculature using structural criteria and high-resolution confocal microscopy. Invest Ophthalmol Vis Sci 2020;61:3.
22. Antcliff RJ, Hussain AA, Marshall J. Hydraulic conductivity of fixed retinal tissue after sequential excimer laser ablation: barriers limiting fluid distribution and implications for cystoid macular edema. Arch Ophthalmol 2001;119:539–544.
23. Antcliff RJ, Marshall J. The pathogenesis of edema in diabetic maculopathy. Semin Ophthalmol 1999;14:223–232.
24. Gaudric A, Audo I, Vignal C, et al. Non-vasogenic cystoid maculopathies. Prog Retin Eye Res 2022;91:101092.
25. Jaffe GJ, Ying G-S, Toth CA, et al. Macular morphology and visual acuity in year five of the comparison of age-related macular degeneration treatments trials. Ophthalmology 2019; 126:252–260.
26. Ramtohul P, Engelbert M, Malclès A, et al. Bacillary layer detachment: multimodal imaging and histologic evidence of a novel optical coherence tomography terminology: literature review and proposed theory. Retina 2021;41:2193–2207.
27. Ramtohul P, Comet A, Denis D, Gascon P. Hemorrhagic bacillary layer detachment in macular telangiectasia type 2. Retina 2021;41:e42–e43.
28. Ramtohul P, Malclès A, Gigon E, et al. Long-term outcomes of bacillary layer detachment in neovascular age-related macular degeneration. Ophthalmol Retina 2022;6:185–195.
29. Doobin D, Sharma T, Horowitz J. Ruptured retinal arterial macroaneurysms associated with hemorrhagic bacillary layer detachments. Retin Cases Brief Rep 2022. doi: 10.1097/ICB.0000000000001371
30. Amoroso F, Mrejen S, Pedinielli A, et al. Intraretinal hyperreflective lines. Retina 2021;41:82–92.